Nano Vision, Vol.1 (3), 129-152 (2011)

Fabrication of Zn-Cd Composite Nano Rods, Knife and Wires by New Method

S. SAKTHIVEL[1] and D. MANGALARAJ[2]

[1]Thinfilm Physics and Nano Science Laboratory,
PG and Research Department of Physics ,
Rajah Serfoji Govt. College, Thanjavur -613 005, Tamilnadu, India
[2]Department of Nano Science and Nano Technology,
Bharathiar University, Coimbatore- 641 046, Tamilnadu , India

ABSTRACT

Zn-Cd composite nano rod (nr), nano knife (nk) and wires (nw) were fabricated simultaneously using new chemical technique . The fabrication temperature involved in this technique is 403 K and identified by FTIR. The nano size samples are prepared by new technique and analysed by XRD. The average size of the these three structure ranging from 10- 69 nm. SEM image gives distribution of nr, nk and nw. The UV and VIS spectrum shows the absorption and transmittance ranging from 0.47 to 50 %. The calculate energy gap value is 2.6eV.

Keywords: Zn-Cd, Zinc, Cadmium, nano rods, nano knife, nano wires.

1. INTRODUCTION

Nanotubes nanowires are getting a lot of attention for variety of electronic applications. Nanotubes are cylinders of carbon atoms, nanowires are tiny wire made from metals such as silver or semiconductor.

Researchers have already created memory devices using nanotubes and nanowires. Eventually the computer industry may be able to replace memory cells that are about a hundred nanometers wide with cells that are only a few nanometers wide. Hewlettpackard recently found a way to use nanowires to construct a device only a few nanometers wide that performs electrical operations normally requiring at least two transistors. This device, a special combination of three nanowires, is calld a crossbar latch.

In nanotechnology, nanorods are one morphology of nanoscale objects. Each of their dimensions range from 1-100 nm. They may be synthesized from metals or semiconducting materials. The applications of nanorods are diverse, ranging from display technologies to microelectro-mechanical systems (MEMS).

Even though cadmium and its compounds may be toxic in certain forms and concentrations, the British Pharmaceutical Codex from 1907 states that cadmium iodide was used as a medication to treat "enlarged joints, scrofulous glands, and chilblains". Dunglison, *et al*., (1866). Cadmium has many common industrial uses as it is a key component in battery production, is present in cadmium pigments Buxbaum, *et al*., (2005), coatings Smith C.J.E, *et al*., (April 20, 1999). and is commonly used in electroplating. Scoullos, *et al.*, (2001).

2. EXPERIMENTS

2.1 Materials used

Basic materials used for fabricating composite nr, nk, nw are Zinc and Cadmium. The properties of these materials are discussed below.

2.1.1 Properties of Zinc Acetate

Zinc Acetate is the chemical compound with the formula $Zn(O_2CCH_3)_2$, which commonly occurs as a dihydrate $Zn(O_2CCH_3)_2(H_2O)_2$. Both the hydrate and the anhydrous forms are colorless solids that are commonly used in chemical synthesis and as dietary supplements. Zinc acetates are prepared by the action of acetic acid on zinc carbonate or zinc metal. In the event of Zinc-Cadmium nanorods was deposited by various methods like Rolling and dry method, Dip and dry method, Drop and dry method and Vapor-Liquid-Solid method.

2.2. Preparation Technique

Zn-Cd Initially 40 gram Zinc acetate was dissolved by 100 millilitre distilled water and 60 gram Cadmium chloride was dissolved by 50 millilitre distilled water and stirred well by using magnetic stirrer for 1 hour each.

Bulk Zinc acetate material of purify 99.9% were taken and dissolved by distilled water. After that the solution containing Zinc particles were stirred for 1 hour. Finally a complete transparent solution containing nano particles were used for preparing Nano Zinc rods by various techniques Dip, Drop, Rolling, VLS.

Initially 68 gram cadmium chloride was dissolved by 50 millilitre distilled water and 42 gram tin chloride was dissolved by 50 milli litre distilled water and stirred well by using magnetic stirrer for 1 hour.

Bulk cadmium chloride material of purify 99.9% were taken and dissolved by distilled water. After that the solution containing cadmium particles were stirred for 1 hour. Finally a complete transparent solution containing nano particles were used for preparing nano cadmium rods by various techniques Dip, Drop, Rolling, VLS.

These two solutions are preperly mixed in the ratio of 10:30 of ZnAc:CdCl respectively by using magnetic stirrer still getting nr,nk and nw.

2.3. Nano rods, knife and wires preparation technique

2.3.1. Dip coating method

Dip coating is a popular way of creating thin films for research purposes. Uniform films can be applied onto flat or

cylindrical substrates. The following five stages involved in the dip coating process.

Immersion: The substrate is immersed in the solution of the coating material at a constant speed (preferably jitter-free).

Start-up: The substrate has remained inside the solution for a while and is starting to be pulled up.

Deposition: The thin layer deposits itself on the substrate while it is pulled up. The withdrawing is carried out at a constant speed to avoid any jitters. The speed determines the thickness of the coating (faster withdrawal gives thicker coating material).

Drainage: Excess liquid will drain from the surface.

Evaporation: The solvent evaporates from the liquid, forming the thin layer. For volatile solvents, such as alcohols, evaporation starts already during the deposition & drainage steps. In the continuous process, the steps are carried out directly after each other. The various stages of dip coating process are shown in the Figure 2.1 (a-d).

2.3.2. Drop method

Ultrasonically cleaned cylindrical metal needle rod were immersed in a beaker containing transparent Zinc Acetate-Cadmium chloride solution. The immersed rod was dropped over an ultrasonically cleaned glass substrate. After pull out the glass plate were kept in the open atmosphere for two to three hours. Finally the required nanorods were obtained and it was apply for further studies. The coated glass plate has only Cadmium particles on the Zinc nano rods and it was conformed by XRD and SEM. The different stages of Drop methods are shown in the Figure 2.2 (a-d).

2.3.3. Rolling method

A well cleaned cylindrical glass rod were immersed in a beaker containing transparent Zinc Acetate-Cadmium chloride solution. The immersed rod was rolled over a well ultrasonically cleaned glass substrate. After taking the glass plate with particle or rod it was kept in the open atmosphere for two to three hours for dry. Finally the required nano rods or particles were prepared and apply for studying various properties. The coated glass with rod or particle of a has only Cadmium and Zinc and it was conformed by XRD and SEM. The different stages of rolling methods are shown in the Fig. 2.3 (a-d)

2.3.4. Vapor-Liquid-Solid method

The vapor-liquid-solid method (VLS) is a mechanism for the growth of one-dimensional structures, such as nanowires, from chemical vapor deposition. Growth of a crystal through direct adsorption of a gas phase on to a solid surface is generally very slow. Three stages of VLS mechanism is illustrated below.

Preparation of a liquid alloy droplet upon the substrate from which a wire is to be grown.

Introduction of the substance to be grown as a vapor, which adsorbs on to the liquid surface, and diffuses in to the droplet.

Supersaturation and nucleation at the liquid/solid interface leading to axial crystal growth.

The VLS process takes place for example growth of Au on Si Substrate are explained below:

1. A thin (~1-10 nm) Au film is deposited onto a silicon (Si) wafer substrate by sputter deposition or thermal evaporation.

2. The wafer is annealed at temperatures higher than the Au-Si eutectic point, creating Au-Si alloy droplets on the wafer surface (the thicker the Au film, the larger the droplets). Mixing Au with Si greatly reduces the melting temperature of the alloy as compared to the alloy constituents. The melting temperature of the Au:Si alloy reaches a minimum (~363°C) when the ratio of its constituents is 4:1 Au:Si, also known as the Au:Si eutectic point.

3. Lithography techniques can also be used to controllably manipulate the diameter and position of the droplets (and as you will see below, the resultant nanowires).

4. One-dimensional crystalline nanowires are then grown by a liquid metal-alloy droplet-catalyzed chemical or physical vapor deposition process, which takes place in a vacuum deposition system.

Following the above procedure finally Zn-Cd composite nanorods and were growned and it was taken for further studies.

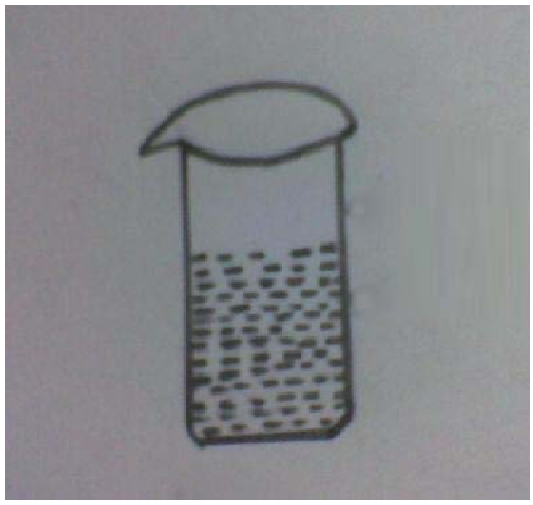

(a)

(b)

Figure 2.1 (a-b). Block diagrams of Dip coating Method

a. Zn-Cd composite solution
b. Glass substrate immersed in the solution

(c)

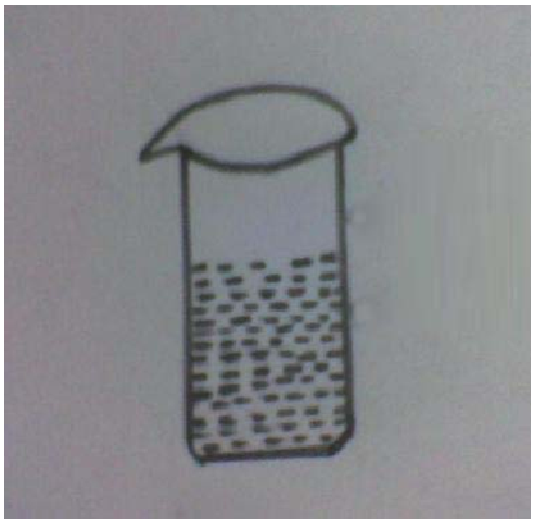

(a)

(d)

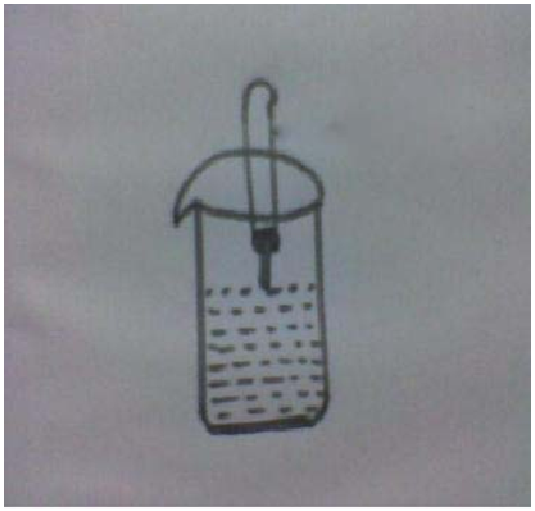

(b)

Figure 2.1 (c-d). Block diagrams of Dip coating Method

c. Glass substrate immersed in the solution

d. Take the substrate from the solution and drying at open atmosphere

Figure 2.2 (a-b) Block diagrams of Drop Method

a. Zn-Cd composite solution

b. Filler inserted in the solution

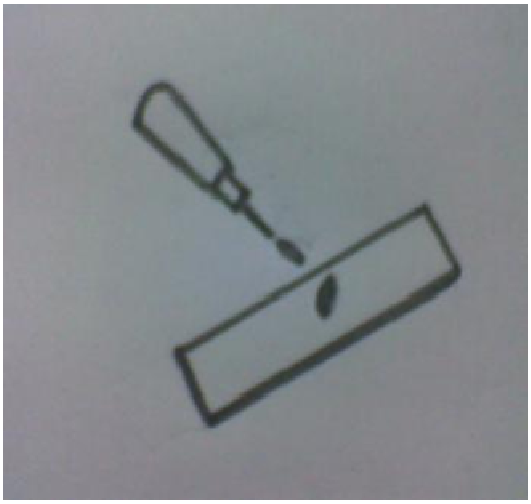

(c)

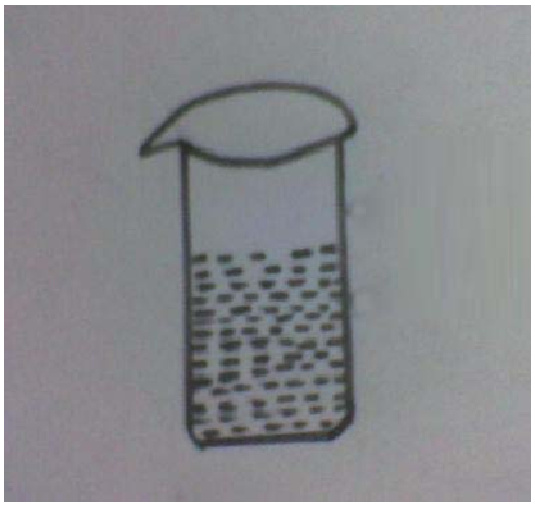

(a)

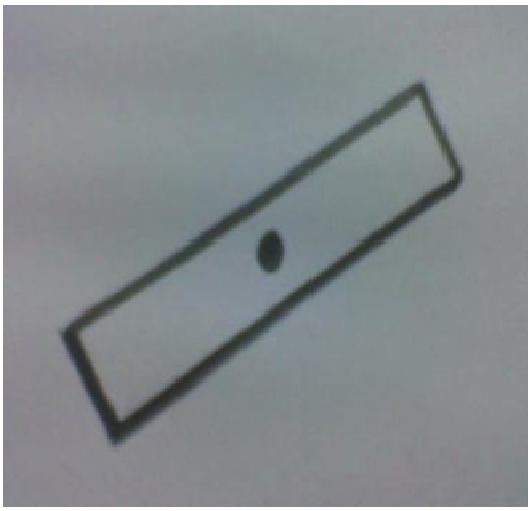

(d)

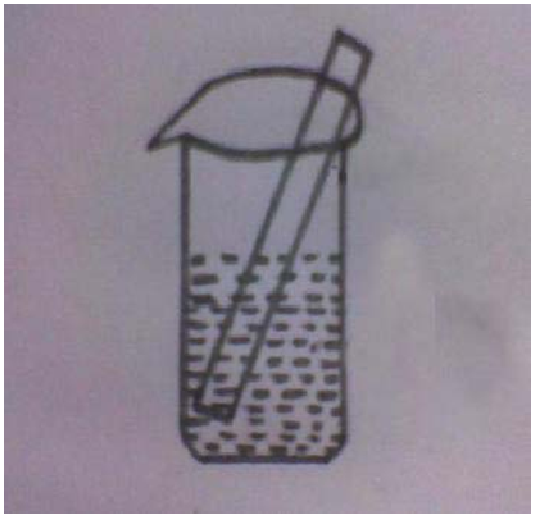

(b)

Figure 2.2(c-d). Block diagrams of Drop Method

c. Press the filler for drop on the well cleaned substrate

d. Zn-Cd composite sample drying at open atmosphere

Figure 2.3 (a-b) Block diagrams of Rolling Method

a. Zn-Cd composite solution

b. Glass rod immersed in the solution

(c)

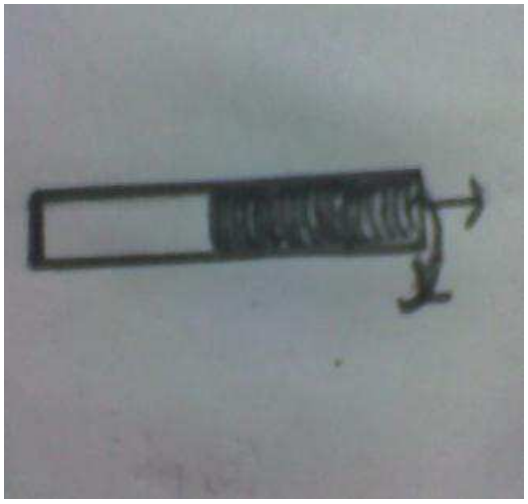

(d)

Figure 2.3 (c-d) Block diagrams of Rolling Method

c. Start up rolling

d. Zn-Cd composite sample

2.4. Sample Analysis

This is the simple example template containing only headers for each report item and the bookmarks. The invisible bookmarks are indicated by text between brackets.

2.4.1. X-Ray Diffraction (XRD)

X-ray scattering techniques are a family of non-destructive analytical techniques which reveal information about the crystallographic structure, chemical composition, and physical properties of materials and thin films.

These techniques are based on observing the scattered intensity of an X-ray beam hitting a sample as a function of incident and scattered angle, polarization, and wavelength or energy.

X-ray diffraction techniques

Crystals are regular arrays of atoms, and X-rays can be considered waves of electromagnetic radiation. Atoms scatter X-ray waves, primarily through the atoms' electrons. Just as an ocean wave striking a lighthouse produces secondary circular waves emanating from the lighthouse, so an X-ray striking an electron produces secondary spherical waves emanating from the electron. This phenomenon is known as elastic scattering, and the electron (or lighthouse) is known as the scatterer.

A regular array of scatterer produces a regular array of spherical waves. Although these waves cancel one another out in most directions through destructive interference, they add constructively in a few specific directions, determined by Bragg's law:

$$2d\sin\theta = n\lambda \quad (2.1)$$

Where ‘d’ is the spacing between diffracting planes, ‘θ‘is the incident angle, ‘n’ is any integer, and ’λ’ is the wavelength of the beam. These specific directions appear as spots on the diffraction pattern called reflections. Thus, X-ray diffraction results from an electromagnetic wave (the X-ray) impinging on a regular array of scatterers (the repeating arrangement of atoms within the crystal).

X-rays are used to produce the diffraction pattern because their wavelength λ is typically the same order of magnitude (1-100 Ångströms) as the spacing d between planes in the crystal.

2.4.2. Scanning Electron Microscope (SEM)

A scanning electron microscope (SEM) is a type of electron microscope that images a sample by scanning it with a high-energy beam of electrons in a raster scan pattern. The electrons interact with the atoms that make up the sample producing signals that contain information about the sample's surface topography, composition, and other properties such as electrical conductivity.

The types of signals produced by an SEM include secondary electrons, back-scattered electrons (BSE), characteristic X-rays, light (cathodoluminescence), specimen current and transmitted electrons. Secondary electron detectors are common in all SEMs, but it is rare that a single machine would have detectors for all possible signals. The signals result from interactions of the electron beam with atoms at or near the surface of the sample. In the most common or standard detection mode, secondary electron imaging or SEI, the SEM can produce very high-resolution images of a sample surface, revealing details about less than 1 to 5 nm in size. Due to the very narrow electron beam, SEM micrographs have a large depth of field yielding a characteristic three-dimensional appearance useful for understanding the surface structure of a sample.

This is exemplified by the micrograph of pollen shown to the right. A wide range of magnifications is possible, from about 10 times (about equivalent to that of a powerful hand-lens) to more than 500,000 times, about 250 times the magnification limit of the best light microscopes. Back-scattered electrons (BSE) are beam electrons that are reflected from the sample by elastic scattering. BSE are often used in analytical SEM along with the spectra made from the characteristic X-rays. Because the intensity of the BSE signal is strongly related to the atomic number (Z) of the specimen, BSE images can provide information about the distribution of different elements in the sample.

For the same reason, BSE imaging can image colloidal gold immuno-labels of 5 or 10 nm diameter which would otherwise be difficult or impossible to detect in secondary electron images in biological specimens. Characteristic X-rays are emitted when the electron beam removes an inner shell electron from the sample, causing a higher energy electron to fill the shell and release energy. These characteristic X-rays are used to identify the composition and measure the abundance of elements in the sample.

In a typical SEM, an electron beam is thermionically emitted from an electron gun fitted with a tungsten filament cathode. Tungsten is normally used in thermionic electron guns because it has the highest melting point and lowest vapour pressure of all metals, thereby allowing it to be heated for electron emission, and because of its low cost. Other types of electron emitters include lanthanum hexaboride (LaB_6) cathodes, which can be used in a standard tungsten filament SEM if the vacuum system is upgraded and field emission guns(FEG), which may be of the cold-cathode type using tungsten single crystal emitters or the thermally-assisted Schottky type, using emitters of zirconium oxide.

The electron beam, which typically has an energy ranging from 0.5 keV to 40 keV, is focused by one or two condenser lenses to a spot about 0.4 nm to 5 nm in diameter. The beam passes through pairs of scanning coils or pairs of deflector plates in the electron column, typically in the final lens, which deflect the beam in the x and y axes so that it scans in a raster fashion over a rectangular area of the sample surface.

When the primary electron beam interacts with the sample, the electrons lose energy by repeated random scattering and absorption within a teardrop-shaped volume of the specimen known as the interaction volume, which extends from less than 100 nm to around 5 µm into the surface. The size of the interaction volume depends on the electron's landing energy, the atomic number of the specimen and the specimen's density.The energy exchange between the electron beam and the sample results in the reflection of high-energy electrons by elastic scattering, emission of secondary electrons by inelastic scattering and the emission of electromagnetic radiation, each of which can be detected by specialized detectors. The beam current absorbed by the specimen can also be detected and used to create images of the distribution of specimen current. Electronic amplifiers of various types are used to amplify the signals which are displayed as variations in brightness on a cathode ray tube. The raster scanning of the CRT display is synchronised with that of the beam on the specimen in the microscope, and the resulting image is therefore a distribution map of the intensity of the signal being emitted from the scanned area of the specimen. The image may be captured by photography from a high resolution cathode ray tube, but in modern machines is digitally captured and displayed on a computer monitor and saved to a computer's hard disk.

2.4.3. UV-Visible Spectrometer

UV Visible Spectroscopy or Ultra Violet-visible spectrophotometry (UV-Vis or UV/Vis) refers to absorption spectroscopy or reflectance spectroscopy in the ultraviolet-visible spectral region. This means it uses light in the visible and adjacent (near-UV and near-infrared (NIR)) ranges. The absorption or reflectance in the visible range directly affects the perceived color of the chemicals involved. In this region of the electromagnetic spectrum, molecules undergo electronic transitions. This technique is complementary to fluorescence spectroscopy, in that fluorescence deals with transitions from the excited state to the ground state, while absorption measures transitions from the ground state to the excited state.

The basic parts of a spectrophotometer are a light source, a holder for the sample, a diffraction grating in a monochromator or a prism to separate the different wavelengths of light, and a detector. The radiation source is often a Tungsten filament (300-2500 nm), a deuterium arc lamp, which is continuous over the ultraviolet region (190-400 nm), Xenon arc lamps, which is continuous from 160-2,000 nm; or more recently, light emitting diodes (LED) for the visible wavelengths. The detector is typically a photomultiplier tube, a photodiode, a photodiode array or a charge-coupled device(CCD). Single photodiode detectors and photomultiplier tubes are used with scanning monochromators, which filter the light so that only light of a single wavelength reaches the detector at one time.

The scanning monochromator moves the diffraction grating to "step-through" each wavelength so that its intensity may be measured as a function of wavelength. Fixed monochromators are used with CCDs and photodiode arrays. As both of these devices consist of many detectors grouped into one or two dimensional arrays, they are able to collect light of different wavelengths on different pixels or groups of pixels simultaneously.

A spectrophotometer can be either single beam or double beam. In a single beam instrument (such as the Spectronic 20), all of the light passes through the sample cell. I_o must be measured by removing the sample. This was the earliest design, but is still in common use in both teaching and industrial labs.

In a double-beam instrument, the light is split into two beams before it reaches the sample. One beam is used as the reference; the other beam passes through the sample. The reference beam intensity is taken as 100% Transmission (or 0 Absorbance), and the measurement displayed is the ratio of the two beam intensities. Some double-beam instruments have two detectors (photodiodes), and the sample and reference beam are measured at the same time. In other instruments, the two beams pass through a beam chopper, which blocks one beam at a time. The detector alternates between measuring the sample beam and the reference beam in synchronism with the chopper. There may also be one or more dark intervals in the chopper cycle. In this case the measured beam intensities may be corrected by subtracting the intensity measured in the dark interval before the ratio is taken.

Samples for UV/Vis spectrophotometry are most often liquids, although the absorbance of gases and even of solids can also be measured. Samples are typically placed in a transparent cell, known as a cuvette. Cuvettes are typically rectangular in shape, commonly with an internal width of 1 cm. Test tubes can also be used as cuvettes in some instruments. The type of sample container used must allow radiation to pass over the spectral region of interest. The most widely applicable cuvettes are made of high quality fused silica or quartz glass because these are transparent throughout the UV, visible and near infrared regions. Glass and plastic cuvettes are also common, although glass and most plastics absorb in the UV, which limits their usefulness to visible wavelengths.

Specialized instruments have also been made. These include attaching

spectrophotometers to telescopes to measure the spectra of astronomical features. UV-visible micro spectrophotometers consist of a UV-visible microscope integrated with a UV-visible spectrophotometer.

A complete spectrum of the absorption at all wavelengths of interest can often be produced directly by a more sophisticated spectrophotometer. In simpler instruments the absorption is determined one wavelength at a time and then compiled into a spectrum by the operator. By removing the concentration dependence, the extinction coefficient (ε) can be determined as a function of wavelength.

It measures the intensity of light passing through a sample (I), and compares it to the intensity of light before it passes through the sample (I_o). The ratio I / I_o is called the transmittance, and is usually expressed as a percentage (%T). The absorbance, A, is based on the transmittance:

$$A = -\log(\%T / 100\%) \quad (2.2)$$

The UV-visible spectrophotometer can also be conFigured to measure reflectance. In this case, the spectrophotometer measures the intensity of light reflected from a sample (I), and compares it to the intensity of light reflected from a reference material (I_o)(such as a white tile). The ratio I / I_o is called the reflectance, and is usually expressed as a percentage (%R).

3.1. RESULT AND DISCUSSION

X-ray diffraction patterns of nr,nk and nw are prepared by using new techniques are presented in Figure 3.1(a-d). The obtained peaks in the diffraction spectra indicates the polycrystalline nature of the nano structures. The peak positions are well matched with Cd X-ray pattern S. Sakthivel *et al*., (2011) other than Zn-Cd composite nano rods, no other by products are found in the pattern S. Sakthivel *et al*., (2011). This indicates that the purity of the Zn-Cd composite nanorods. If we go further with high temperature and time treatment there is a possibility or getting good crystallinity. From this finding it is important that the hydrothermal treatment temperature and time are very important to get pure phase of Zn-Cd composite with required important crystallinity.

The d spacing value of the nano crystal varying from 8.0627 Å to 1.241 Å calculated the lattice parameter of the hydro thermally synthesized Zn-Cd composite nanorods / nano particles as 8.062 Å using multiple XRD peaks and least-squares method, which is with in the range of previously reported values. No peaks originating from impurities could be seen indicating the formation of pure Zn-Cd composite nanorods composites. The average nano rod size calculated from the X-ray diffraction for the as prepared Zn-Cd composite rods was 29.316 nm and ranging from 10.35 nm to 69.19 nm more than 32 peaks were observed due to the contribution of Zn-Cd composite nanorods in Figure 3.2. The 2θ, flex width, d- spacing intensity and I/I_0 value of the X-ray were listed in Table 3.1.

The d spacing value and full wave half maximum(FWHM) for each crystalline size were given in the Table 3.2. Crystalline size of the nanorods were calculated using Debye-Sherrer formula,

$$D = k\lambda / \beta\cos\theta \quad (3.1)$$

Where,

K is the particle shape factor (0.827),
λ is the wavelength of the X-ray used,
β is the calibrated half intensity width of the selected diffraction peak,
θ is the Bragg's angle.

Using the above formula, we calculated the average grain size is 29.316 nm.

UV-Visible Spectroscopy was used to characterize the optical absorptions of Zn-Cd composite nanorods. It is well known that theory of optical absorption gives the relationship between the absorption coefficients 'α' and photon energy 'hν' for direct allowed transition as

$$(\alpha h\nu)^2 = B(h\nu - E_g) \quad (3.2)$$

Where,

hν is the photon energy,
E_g is the apparent optical band gap,
B is the semiconductor characteristic constant,
α is the absorption coefficient.

The optical band gap for the absorption edge can therefore be obtained by extrapolating the linear potion of $(\alpha h\nu)^2$ - hν to α=0.

The dotted lines show the linear fit and corresponding extrapolation. The E_g values for Zn-Cd composite nanorods are 2.6 eV proposed that the increase in the band gaps of the Zn-Cd composite nanorods are indicative of quantum confinement effects, arising owing to their small size. The authers have also attributed the increase in the band gap to quantum confinement effects.

Figure 3.4. and 3.5. shows the absorption versus wavelength and transmittance versus wavelength respectively of the Zn-Cd composite nanorods and this due to cluster of nanorods and bundles of nanorods. Reflectance of the sample more than 90% than absorption and transmittance and the calculated value of reflectance were tabulated in Table 3.3.

Figure 3.6. shows the $(\alpha h\nu)^2$ versus hν curves of Zn-Cd composite nanorods prepared by new method at 130 ºC temperature.

The morphologies of the Zn-Cd composite nano structures were characterized by Scanning Electron Microscope (SEM). Figure 3.3. shows the detailed morphologies of the Zn-Cd composite nanorods. From the Figure it is clear that the Zinc crystals are spreaded over the sides of the Cadmium nanorods and it is clusters randomly distributed over the substrate. The outer diameter of the Cd nanorods ranging from 400 nm to 900 nm prepared at 130ºC SEM analysis for the samples synthesized under new methods. Show the influence of the hydrothermal morphologies. The morphology of the Zn-Cd composite nano structures depends on the hydrothermal conditions i.e. temperature, but the reaction time not influence the morphology of the samples.

Zinc–Cadmium (Zn-Cd) rods successfully fabricated by New method, and the prepared Zn-Cd rods were enlarged by scanning Electron microscope (SEM) Fig. 3.3. (a-e) shows the enlarged image of Zn-Cd nanorods in 5μm to 100 μm range.

Fig. 3.3. (a) shows the parallel Zn-Cd nanorods of length more than 5000 nm and its breadth closely 500 nm using the new method it is also possible to bring down the breadth of the Zn-Cd nanorods. Also from the Figure it is clear that the Zn-Cd rods are perfect parallel and uniform breadth. The edges of the rods or like knife having uniform sharpness on both sides of the rods / knife. The growth direction also possible to control by New method. After particular length of the Zn-Cd nanorods the growth of the rods breadth little bit increased also seen in the same Figure. In addition to that the single bundle of the Zn-Cd nanorods with the distance of each of the order of 10^{-10}m.

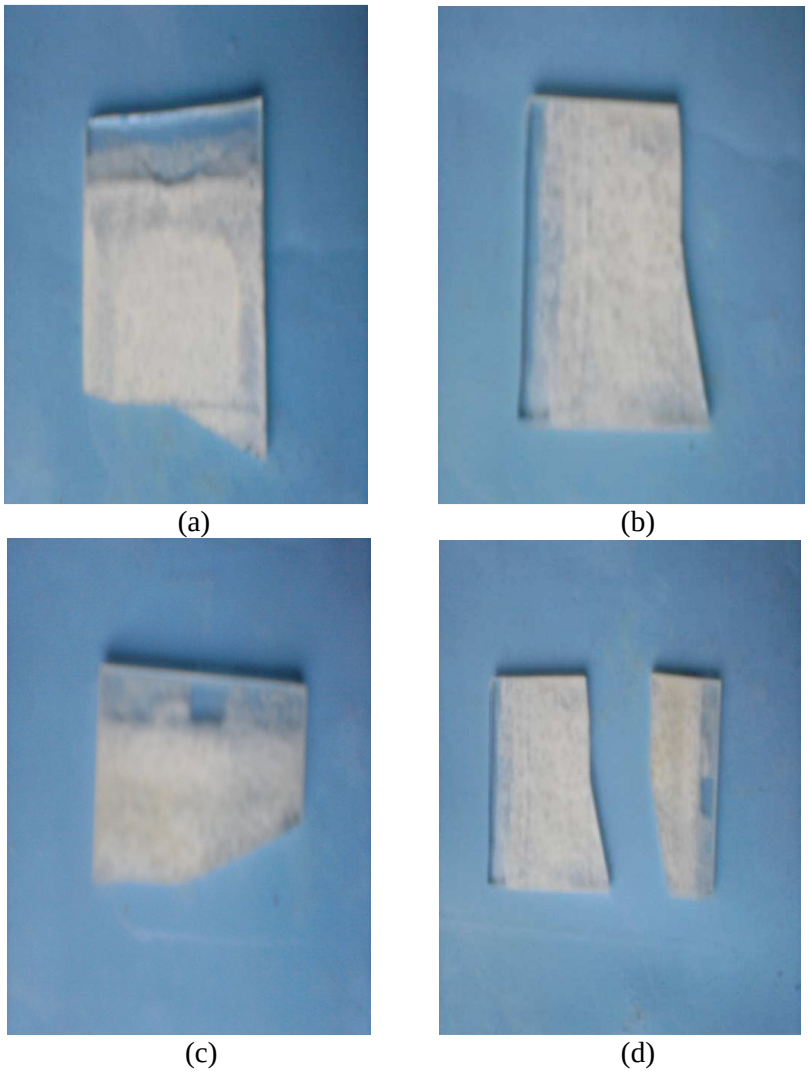

Figure 3.1(a-d) As prepared Zn-Cd composite nr,nk & nw on glass plate.

Fig. 3.3. (b) shows the number of bundles of Zn-Cd nanorods growth separated each by 10^{-10}m. A average single bundle of Zn-Cd nanorods of with 10μm are seen in the same Figure. From the growth origin the rods are looking like sun rays emitted from the semi sphere. Along with this the distance between the each rods increased gradually form the growth origin. A perfect cylindrical Zn-Cd nanorods are displayed in Figure 3.3. (c) in the same Figure it is clear that the rods are little bit smoother in particular area and knife like [fig. 3.3. (b)] in another area. The above contradiction due to the major advantages of the new method.

Growth of Zn-Cd nanorods are clearly pictured in fig. 3.3 (d). Using the same method if we grow the same in other metal seed rods for further applications. The growth direction indicates that all possible numbers of Zn-Cd nanorods is possible simultaneously by this new method. i.e. single rods alone, double rods, triple rods etc. But the growth direction different for different set of Zn-Cd nanorods grown at 130^0C.

Cylindrical type Zn-Cd nanorods and plate type nanorods are simultaneously prepared. By this new method is illustrated in Fig 3.3(e) In addition to that Zn-Cd nanowires are also fabricated and it is shown in fig 3.3. (e).The grain size and band gap energy values are calculated using 'c' programme are given below.

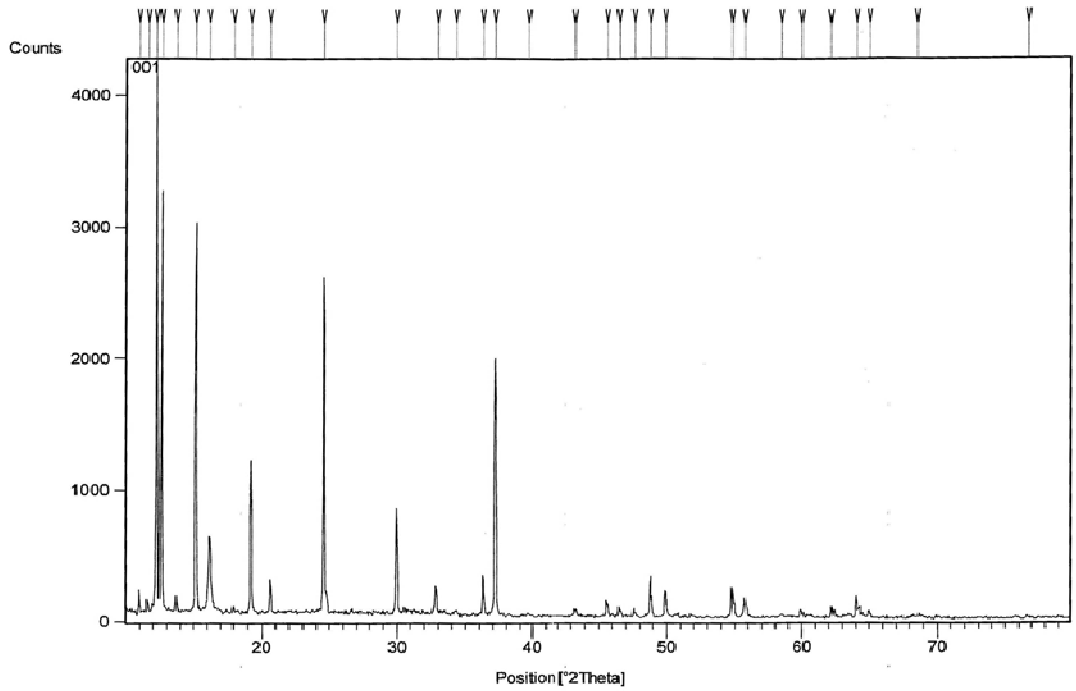

Figure 3.2. XRD Pattern of Zn-Cd composite nr,nk & nw

Table 3.1. d- spacing values of nr,nk & nw

Pos. [°2Th.]	Height [cts]	FWHM [°2Th.]	d-spacing [Å]	Rel. Int. [%]
10.9645	152.63	0.1204	8.06277	3.56
11.5333	75.02	0.3700	7.66640	1.75
12.2195	4287.31	0.0606	7.23740	100.00
12.5594	2711.89	0.0707	7.04230	63.25
13.6995	123.02	0.0941	6.45865	2.87
15.1464	2686.73	0.0813	5.84478	62.67
16.1860	574.19	0.2363	5.47165	13.39
17.9432	62.22	0.1476	4.94366	1.45
19.2105	1036.32	0.0854	4.61646	24.17
20.6714	263.35	0.0980	4.29338	6.14
24.5328	2523.63	0.0842	3.62566	58.86
29.9495	723.13	0.0698	2.98111	16.87
32.9251	105.81	0.4947	2.71818	2.47
34.2736	28.09	0.5459	2.61425	0.66
36.2845	305.77	0.1001	2.47385	7.13
37.1242	2014.91	0.1060	2.41980	47.00
39.6408	23.60	0.5151	2.27178	0.55
43.2394	56.46	0.1823	2.09068	1.32
45.5456	125.49	0.0914	1.99004	2.93
46.4615	73.58	0.1073	1.95292	1.72
47.5316	68.29	0.0884	1.91142	1.59
48.7548	282.17	0.0857	1.86628	6.58
49.8474	199.78	0.0964	1.82790	4.66
54.8413	208.83	0.1019	1.67267	4.87
55.7691	136.21	0.1412	1.64702	3.18
58.4161	26.45	0.2828	1.57854	0.62
59.9103	58.60	0.2460	1.54397	1.37
62.0751	99.52	0.1187	1.49399	2.32
64.0366	134.26	0.1736	1.45287	3.13
64.9418	49.12	0.1517	1.43479	1.15
68.5333	24.84	1.3190	1.36810	0.58
76.7251	20.23	1.2143	1.24115	0.47

Table 3.2. Grain size of Zn-Cd Composite nr,nk & nw

Peak No.	Angle (θ)	Flex Width (β)	D= κλ /βcosθ Nm	$\delta = 1/D^2$ lines/meter
1	5.4825	0.0602	22.746	1.9328
2	5.7666	0.185	69.193	0.208
3	6.1097	0.0303	42.280	0.559
4	6.2797	0.0353	36.388	0.755
5	6.8497	0.0470	27.330	1.3388
6	7.5732	0.0406	31.68	0.996
7	8.093	0.1181	10.894	8.42
8	8.9716	0.0738	17.470	3.276
9	9.6052	0.0427	30.25	1.092
10	10.335	0.049	26.42	1.432
11	12.266	0.0421	30.964	1.043
12	14.974	0.0349	37.780	0.70
13	16.462	0.24735	53.692	0.34
14	17.136	0.2729	48.83	0.419
15	18.142	0.0500	26.812	1.39
16	18.562	0.053	25.370	1.553
17	19.820	.2575	52.58	0.361
18	21.619	0.0911	15.05	4.419
19	22.772	0.0457	30.22	1.094
20	23.230	0.0536	25.83	1.498
21	23.765	0.0442	31.602	1.001
22	24.377	0.0428	32.63	0.93
23	24.923	0.0482	29.143	1.17
24	27.420	0.0509	28.30	1.24
25	27.884	0.0706	20.54	2.37
26	29.208	0.1414	10.35	9.335
27	29.955	0.123	11.95	7.00
28	31.037	0.05935	25.070	1.59
29	32.018	0.0868	17.32	3.33
30	32.470	0.0758	19.18	2.718
31	34.266	0.6545	23.54	1.80
32	38.362	0.6071	26.75	1.396

Determination of grain size 'D' using C program :

Formula :

$$D = \kappa\lambda/\beta\cos\theta$$

Program :

```
#include<stdio.h>
#include<conio.h>
#include<math.h>
void main()
{
        float k=0.827;
        float lam=1.524*10^(-10);
        float d,beta,theta;
        clrscr();
        printf(" Enter the beta and theta value :\n");
        scanf("%f%f",&beta,&theta);
        d=((k*lam)/(beta*cos(theta));
        printf("The Grain Size=%f",d);
        getch();
    }
```

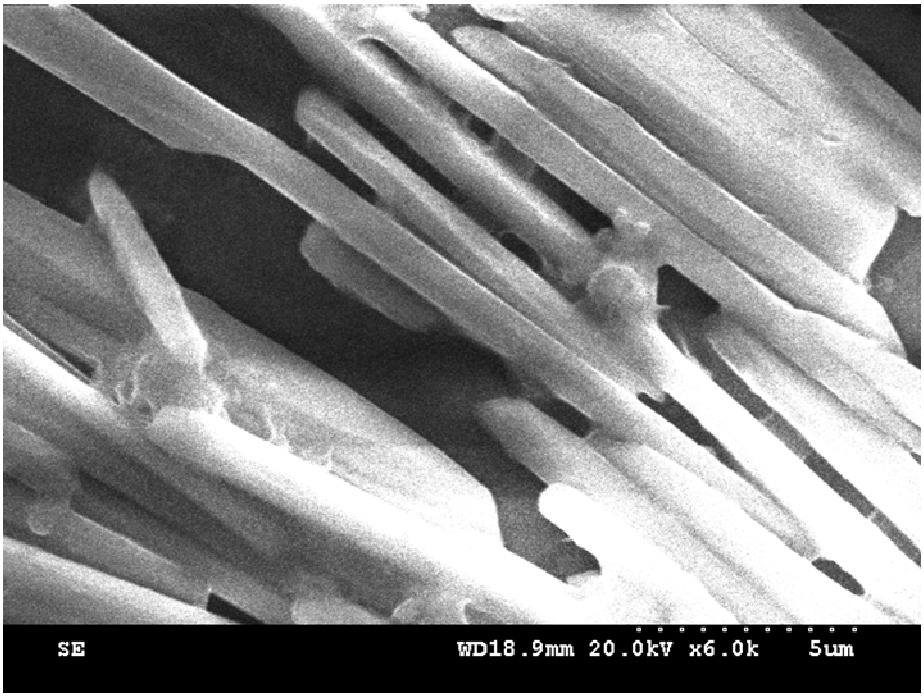

Figure : 3.3 (a) SEM Pattern of Zn-Cd composite nano knife

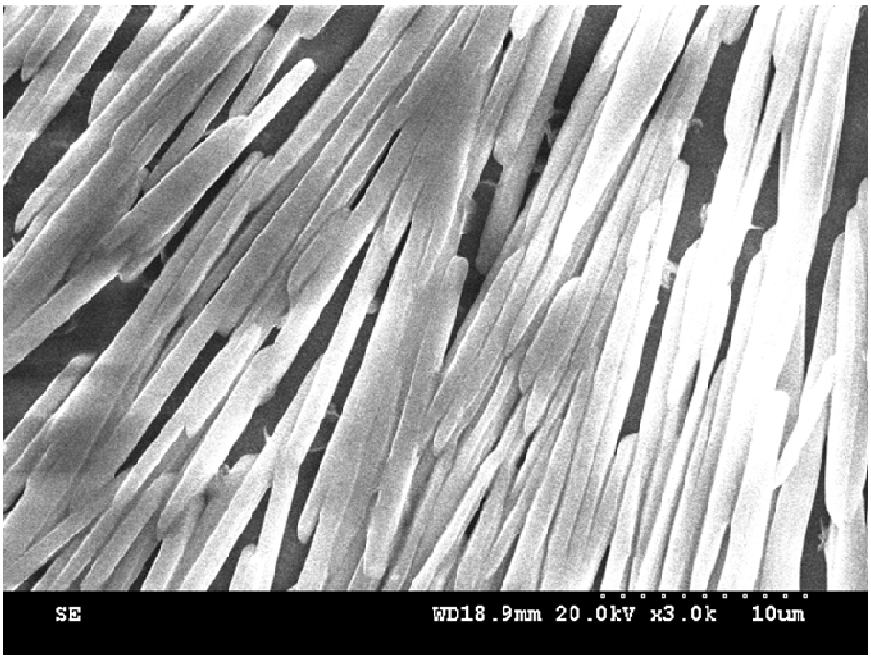

Figure: 3.3(b) SEM Pattern of Zn-Cd composite nano knife.

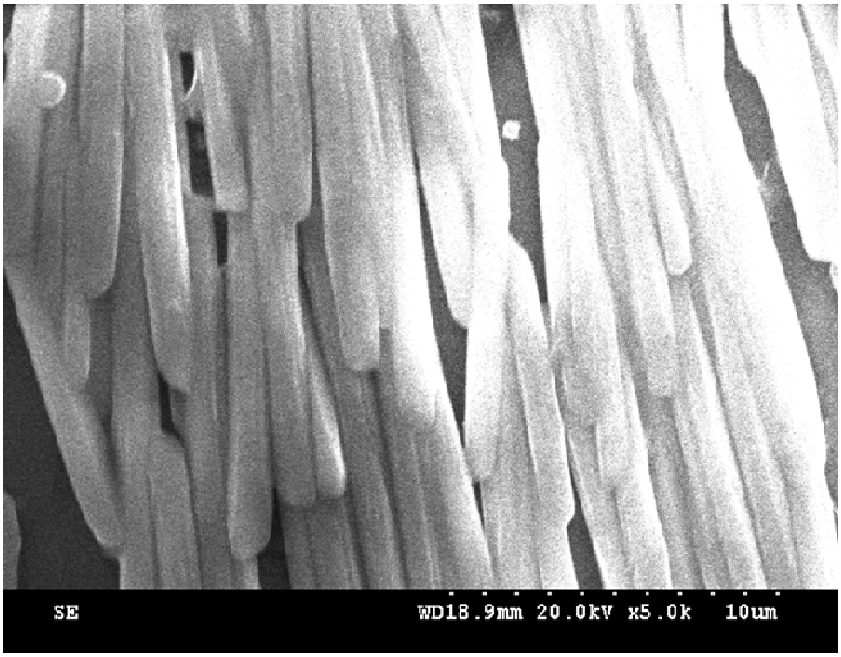

Figure: 3.3(c) SEM image of Zn-Cd composite nano rods.

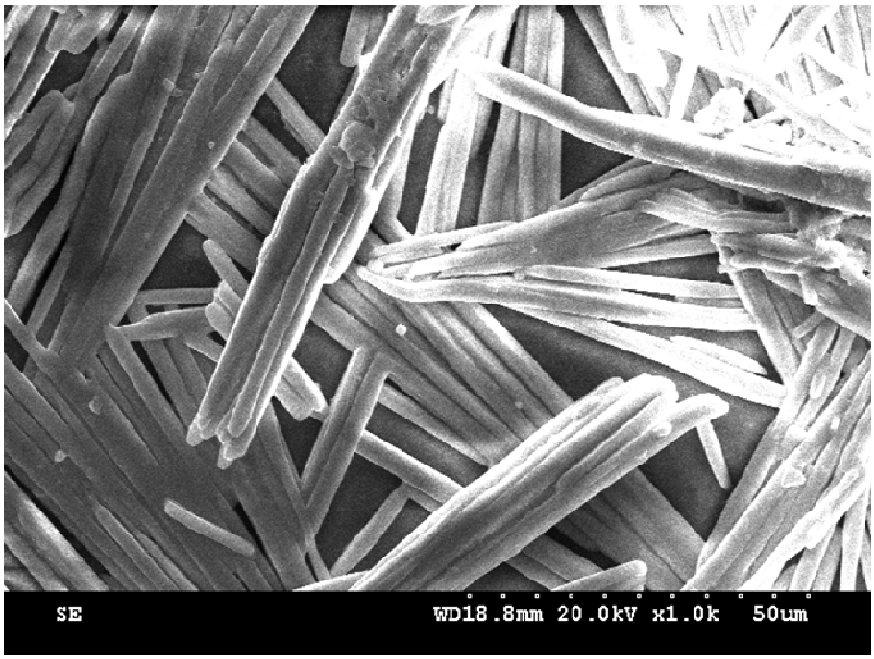

Figure: 3.3(d) SEM Picture of Zn-Cd composite nano knife

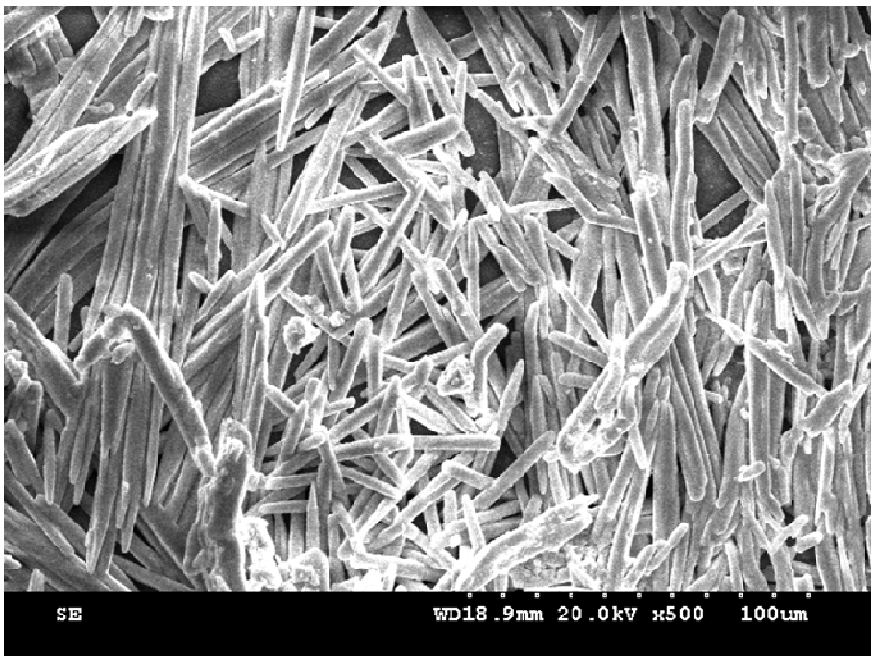

Figure: 3.3(e) SEM Pattern of Zn-Cd composite nano knife (left) rods (center), nano wires (right)

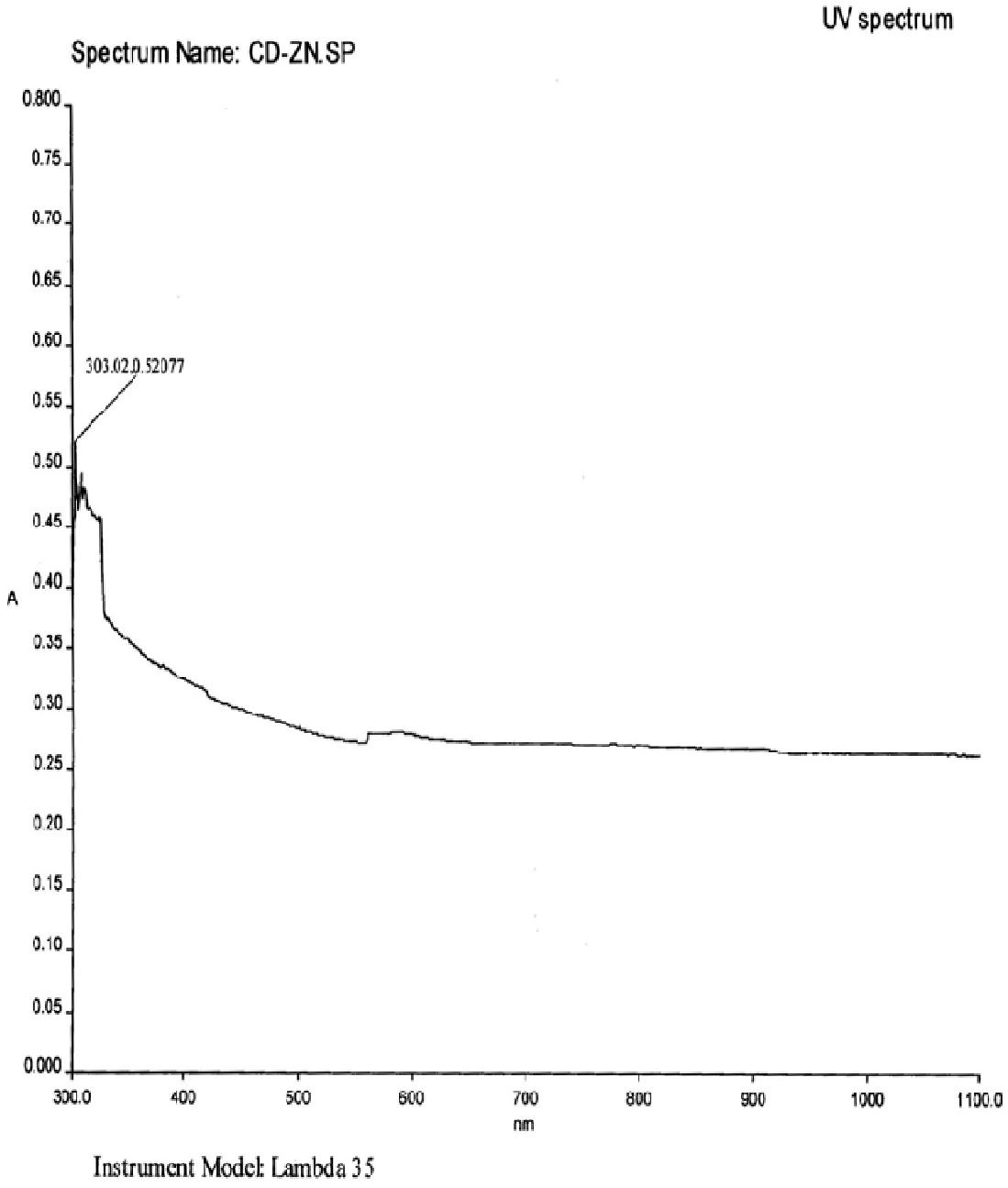

Figure 3.4. UV-Visible Absorption spectrum of Zn-Cd composite nr,nk & nw.

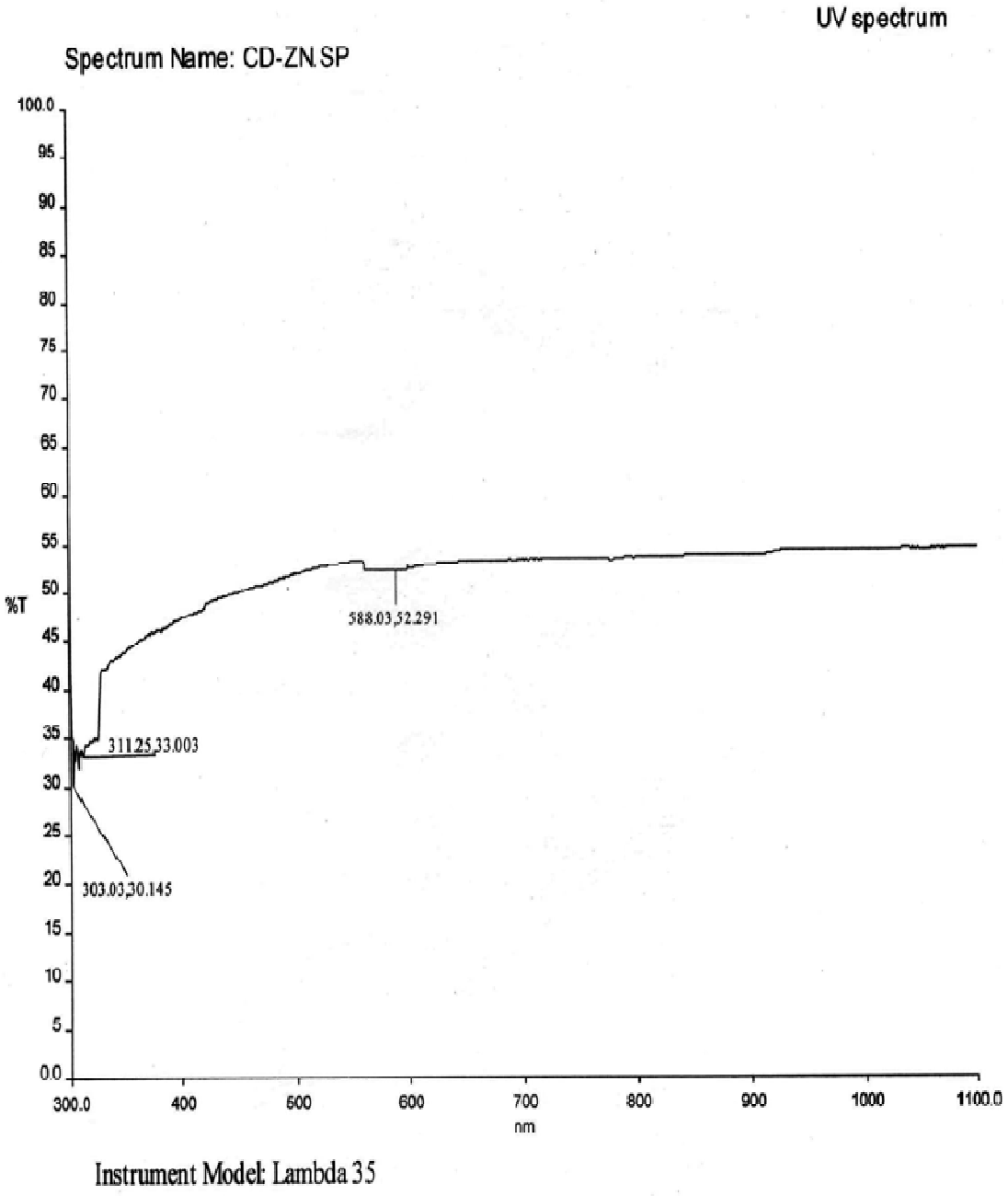

Figure 3.5. UV-Visible Transmission spectrum of Zn-Cd composite nr,nk & nw.

Table 3.3 Absorption, Transmission, Reflection percentage of Zn-Cd composite nr,nk & nw.

Wavelength in nm	Absorptionin %	Transmission %	Reflection in %
400	32	46	22
500	30	53	17
600	29	53	17
700	27	52	21
800	26	53	21
900	27	53	20
1000	26	54	20
1100	26	54	20

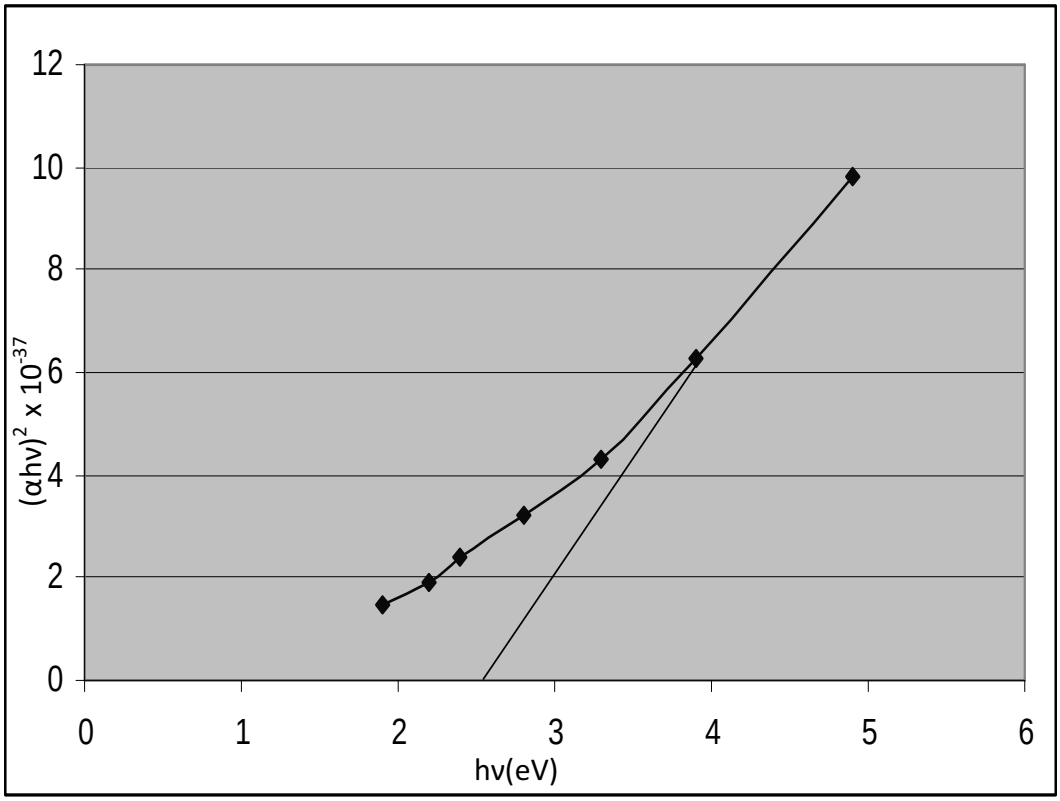

Figure 3.6 Energy band gap diagram of Zn-Cd composite nr,nk & nw

Calculation of band gap energy(Eg) using C program :

Formula :

$$(\alpha h\nu)^2 = B(h\nu - E_g)$$

Program :

```
#include<stdio.h>
#include<conio.h>
#include<math.h>
void main()
{
        float a=2;
        float h=6.626*10^(-34);
        float v,e;
        clrscr();
        printf(" Enter the v value :\n");
        scanf("%f",&v);
        e=sqrt(a*h*v)/(h*v);
        printf("\nThe energy Band gap value=%f",e);
        getch();
 }
```

4. CONCLUSION

Zn-Cd nano rods / knife / wires were successfully fabricated by new method. Using these novel technique it is possible to synthesis nano rods (nr), nano knife (nk) and nano wires (nw) simultaneously.

Zn-Cd nano rods, nano knife / nano wires were synthesized by the new method. The new techniques totally different from the existing method. In addition to the preparation of nr, nk and nw are the clusters on single glass plate. These nano structure are fabricated at 130 ^{0}C by the above techniques.

X – ray diffraction (XRD) peaks indicates the diffraction of x-ray no nr, nk and nw. More then thirty two peaks we found and these are the combination of Zn-Cd nano composites. The average size of the nano rods is 29.316 nm and the rods size ranging from 10.35 nm to 69.19 nm. The d-spacing value of the nanorods varying from 1.241Á to 8.062 Á. The Dislocation Density

values changing from 1.3 x 10^{18} – 9.335 x 10^{18} m^{-1}.

Scanning electron microscope (SEM) image of shows Zn-Cd nr, nk and nws. The cluster of nr, nk and nws distributed and its top view were presented. Separations of these nano structures were possible using SEM. The equality of this new method is simultaneous preparation of nr, nk and nws at 130 ^{o}C.

The UV and visible spectrum of Zn-Cd nr, nk, and nw s where presented and its absorption Á and transmittance percentage are 0.47 and 55% respectively. The calculated band gap energy values of the above nano structure composite material is 2.6 eV .

The Zn-Cd nr, nk and nws are very useful for sensor applications, solar cells fabrication and degradation of toxic liquids.

REFERENCES

1. Buxbaum, Gunter; Pfaff, Gerhard. "Cadmium Pigments". Industrial inorganic pigments. *Wiley-VCH*. pp. 121–123 (2005).
2. Capilla, A.V.; Aranda, R.A. "Anhydrous Zinc(II) Acetate $(CH_3\text{-}COO)_2Zn$". *Crystal Structure Communications* 8: 795–797 (1979).
3. Coombs RRH, Robinson DW, Nanotechnology in Medicine and the Biosciences, by. (1996).
4. Dunglison, Robley Medical Lexicon: A Dictionary of Medical Science. Henry C. Lea. pp. 159 (1866).
5. Freitas RA Jr."What is Nanomedicine?". Nanomedicine: Nanotech. Biol.Med.1 (1):2–9.doi:10.1016/j.nano.2004.11.003 (2005).
6. Hambidge, K. M. and Krebs, N. F. "Zinc deficiency: a special challenge". *J. Nutr*. 137 (4): 1101 (2007).
7. John Wiley & Sons. "Cadmium". Kirk-Othmer Encyclopedia of Chemical Technology. 5 (4-th edition ed.). New York (1994).
8. Katherine Bourzac. "The Feel of Cancer Cells". *Technology Review. MIT*. (December 4, 2007).
9. Martin Stolz, *et al*. Early detection of aging cartilage and osteoarthritis in mice and patient samples using atomic force microscopy, Nature Nanotechnology 4, 186 (2009).
10. Michael Fitzgerald. "Nanobiomechanics". *Technology Review. MIT*. (March/ April 2006).
11. Mozafari, M. R. (ed), Nanocarrier Technologies: *Frontiers of Nanotherapy* (Chapters 1 and 2) pages 10-11, 25-34 (2006).
12. Rowbotham, Thomas Leeson. The art of landscape painting in water colours, by T. and T. L. Rowbotham. p.10 (1850).
13. Scoullos, Michael J.; Vonkeman, Gerrit H.; Thornton, Iain; Makuch, Zen. Mercury, Cadmium, Lead: Handbook for Sustainable Heavy Metals Policy and Regulation. Springer (2001).
14. Smith C.J.E., Higgs M.S., Baldwin K.R. "Advances to Protective Coatings and their Application to Ageing Aircraft". RTO MP-25 (April 20, 1999).
15. J. N. van Niekerk, F. R. L. Schoening and J. H. Talbot. "The crystal structure of zinc acetate dihydrate, $Zn(CH_3COO)_2{\cdot}2H_2O$". *Acta Cryst*. 6 (8): 720–723 (1953).
16. Wagner V, Dullaart A, Bock AK, Zweck A. "The emerging nanomedicine landscape". *Nat Biotechnol*. 24 (10) (2006).